

Electronic supplementary information (ESI) available

## **Self-Assembled Mesoporous Co and Ni-Ferrite Spherical Clusters Consisting of Spinel Nanocrystals Prepared using a Template-Free Approach**

Byong Yong Yu and Seung-Yeop Kwak\*

Department of Materials Science and Engineering, Seoul National University,  
599 Gwanak-ro, Gwanak-gu, Seoul, 151-744, Korea.

\* To whom correspondence should be addressed. *E-mail*: sykwak@snu.ac.kr.

*Tel*: +82-2-880-8365, *Fax*: +82-2-885-1748

**Table S1.** FWHM values of the main diffraction peaks and the crystallite size for M-CoFe<sub>2</sub>O<sub>4</sub> with the respective diffraction planes.

h	k	l	2 $\theta$ (deg.)	<i>d</i> -spacing (nm)	Intensity (a.u.)	FWHM (2 $\theta$ )	Crystallite size (nm)
1	1	1	18.10	0.48	22.9	1.16	6.85
2	2	0	30.14	0.29	32.5	1.28	6.35
3	1	1	35.44	0.25	100.0	1.12	7.36
4	0	0	42.98	0.21	22.6	1.16	7.28
4	2	2	53.54	0.17	13.0	1.64	5.36
5	1	1	57.00	0.16	27.7	1.60	5.58
4	4	0	62.64	0.15	36.8	1.44	6.38

**Table S2.** FWHM values of the main diffraction peaks and the crystallite size for M-NiFe<sub>2</sub>O<sub>4</sub> with the respective diffraction planes.

h	k	l	2 $\theta$ (deg.)	<i>d</i> -spacing (nm)	Intensity (a.u.)	FWHM (2 $\theta$ )	Crystallite size (nm)
1	1	1	17.98	0.48	32.4	1.60	4.97
2	2	0	30.06	0.29	43.3	1.48	5.50
3	1	1	35.42	0.25	100.0	1.48	5.57
4	0	0	42.92	0.21	30.7	1.04	8.12
4	2	2	53.30	0.17	15.9	1.62	5.53
5	1	1	56.74	0.16	31.7	1.00	8.93
4	4	0	62.48	0.15	42.0	1.56	5.89

**Table S3.** The physical properties of as-synthesized mesoporous ferrite clusters (as-M-CoFe<sub>2</sub>O<sub>4</sub> and as-M-NiFe<sub>2</sub>O<sub>4</sub>).

Samples	Cluster size (nm) <sup>a</sup>	Surface area (m <sup>2</sup> g <sup>-1</sup> )	Pore diameter (nm)	Pore volume (cm <sup>3</sup> g <sup>-1</sup> )
as-M-CoFe <sub>2</sub> O <sub>4</sub>	162	103	3.42	0.14
as-M-NiFe <sub>2</sub> O <sub>4</sub>	167	111	3.39	0.12

a: the mean ferrite cluster size was measured using DLS

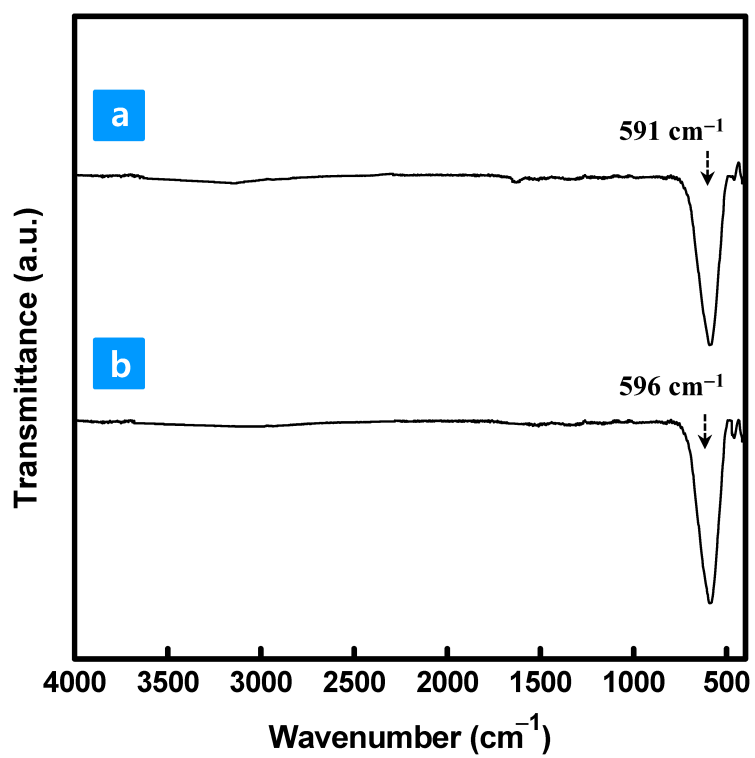


**Fig. S1** FT-IR spectra of (a) M-CoFe<sub>2</sub>O<sub>4</sub> and (b) M-NiFe<sub>2</sub>O<sub>4</sub>.

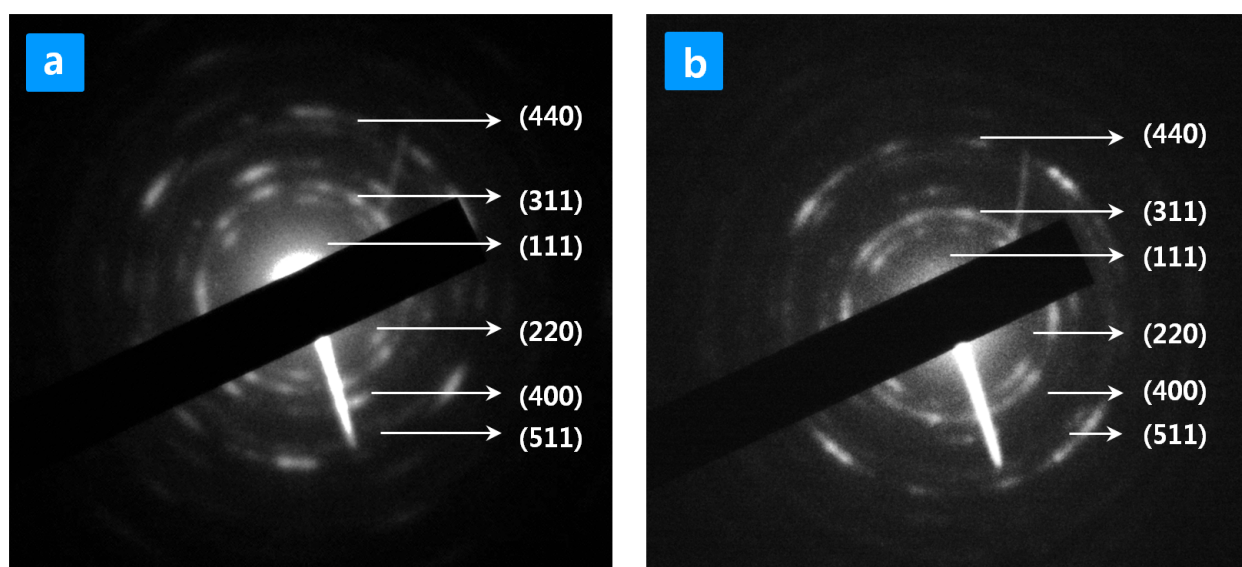


**Fig. S2** Selected area electron diffraction (SAED) patterns acquired from a particular (a) M-CoFe<sub>2</sub>O<sub>4</sub> and (b) M-NiFe<sub>2</sub>O<sub>4</sub> cluster.

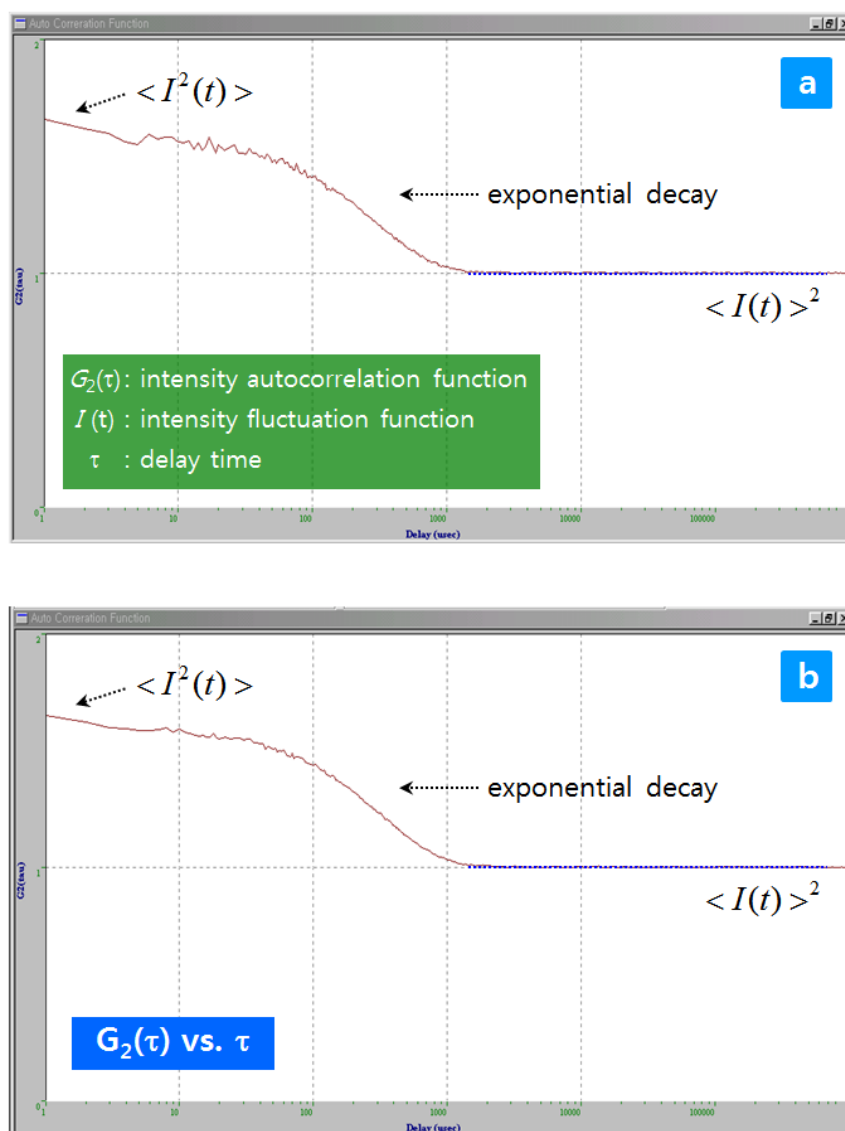


**Fig. S3** The intensity auto-correlation function (ACF),  $G_2(\tau)$  for (a) M-CoFe<sub>2</sub>O<sub>4</sub>, (b) M-NiFe<sub>2</sub>O<sub>4</sub> samples in DLS.

The second-order correlation function  $G_2(\tau)$  can be expressed as a function of the first-order correlation function  $G_1(\tau)$  according to the Siegert relation:  $G_2(\tau) = B(1 + \beta G_1(\tau)^2)$ , where  $B$  is the baseline constant and  $\beta$  is a coherence constant. In the case of a perfect setup, both equal unity. In the case of single-exponential decay,  $G_1(\tau)$  can be expressed in terms of a typical decay rate  $\Gamma$  and time  $t$ ;  $G_1(\tau) = \exp(-\Gamma \tau)$ .

The apparent translational diffusion coefficient,  $D$ , is given by equation:  $\Gamma = Dq^2$ , where  $q$  is the magnitude of the scattering vector  $q = 4\pi n \sin(\theta/2) / \lambda$ , where  $n$  is the refractive index of the solvent,  $\theta$  is the scattering angle, and  $\lambda$  is the wavelength of the incident light. For spherical particles, the translational diffusion coefficient can be related to the hydrodynamic radius,  $R$ , according to the Stokes-Einstein equation:  $D = k_B T / 6\pi\eta R$ , where  $D$  is the diffusion coefficient of the Brownian motion of spherical particles,  $k_B$  is the Boltzmann constant,  $T$  is the absolute temperature, and  $\eta$  is the viscosity of the solvent. The hydrodynamic radius distribution of particles,  $G(R)$  was estimated using the COTIN algorithm, which is conventionally used to determine the inverse Laplace transform of the measured amplitude autocorrelation function.<sup>1,2</sup>

- (1) R. Finsy, *Adv. Colloid Interfac.* 1994, **52**, 79.
- (2) I. K. Voets, A. De Keizer, M. A. Cohen Stuart and P. De Waard, *Macromolecules* 2006, **39**, 5952.

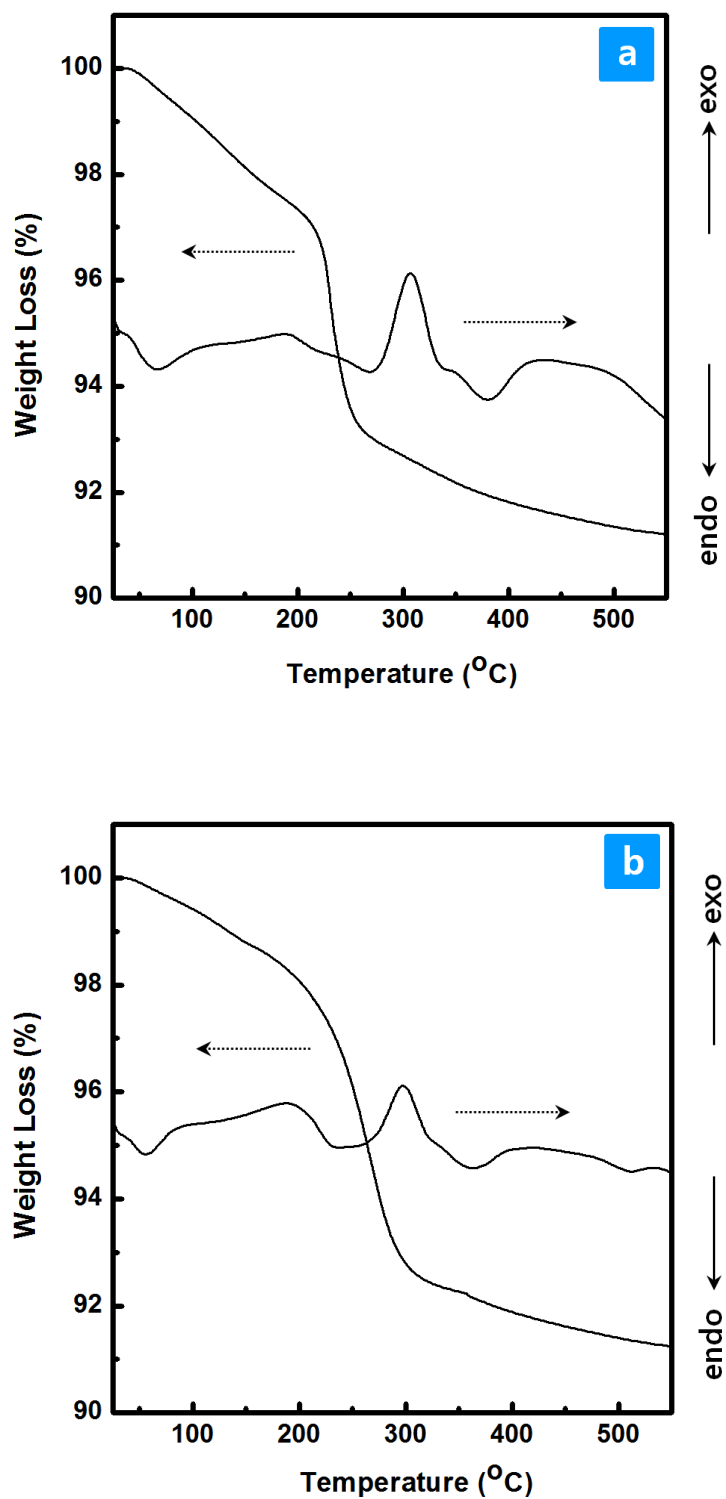


**Fig. S4** TGA and DSC curves of as-prepared (a) M-CoFe<sub>2</sub>O<sub>4</sub> and (b) M-NiFe<sub>2</sub>O<sub>4</sub> before calcination.

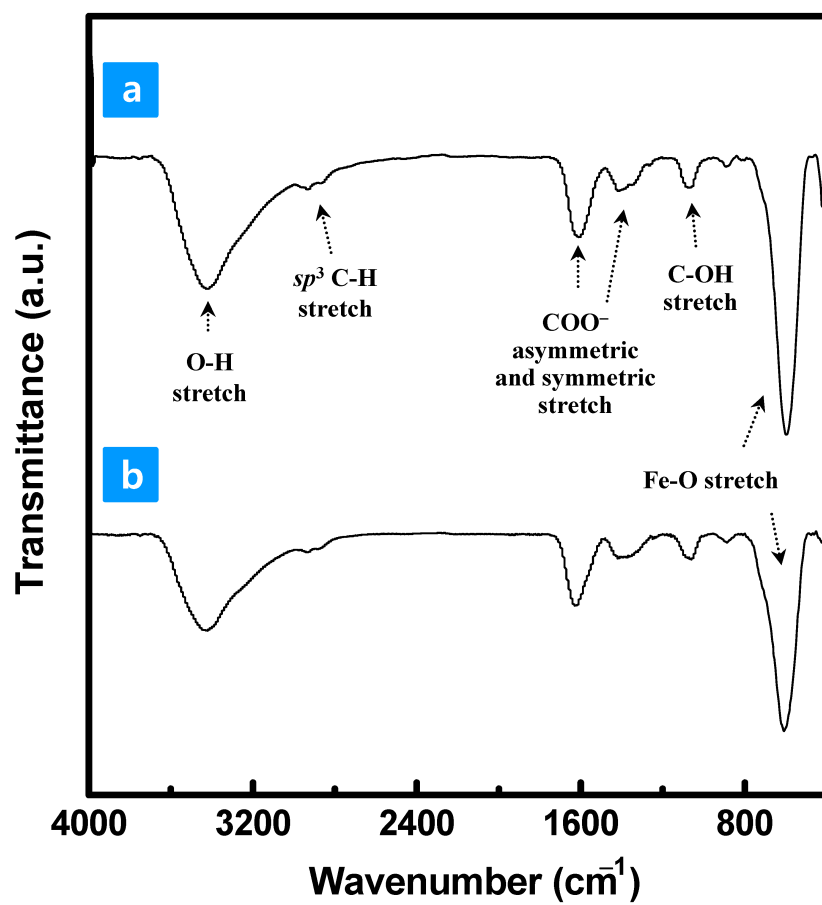


**Fig. S5** FT-IR spectra of as-synthesized (a) M-CoFe<sub>2</sub>O<sub>4</sub> and (b) M-NiFe<sub>2</sub>O<sub>4</sub> before calcination.

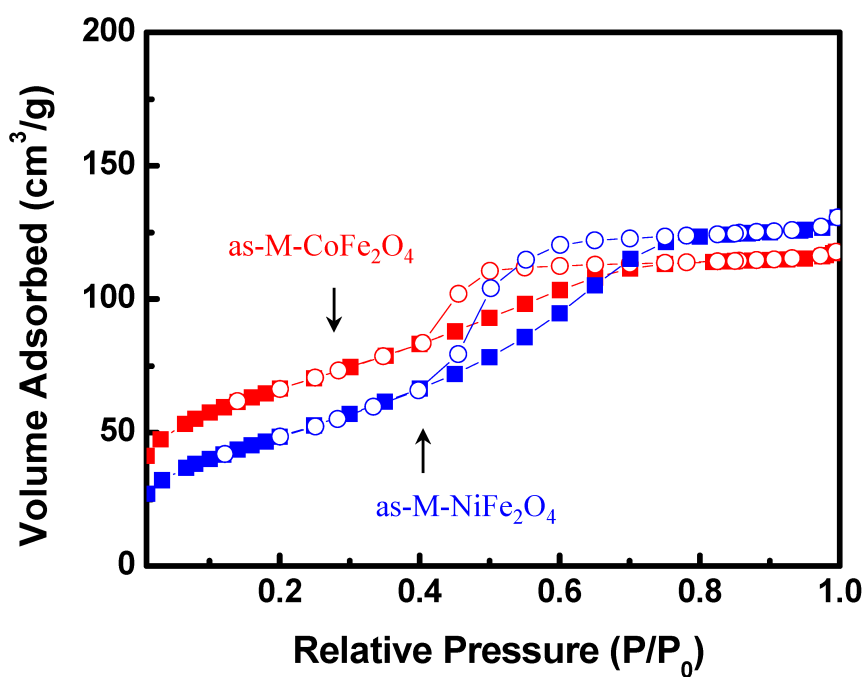


**Fig. S6** N<sub>2</sub> adsorption(■) -desorption(○) isotherms for as-synthesized (a) M-CoFe<sub>2</sub>O<sub>4</sub> and (b) M-NiFe<sub>2</sub>O<sub>4</sub>.

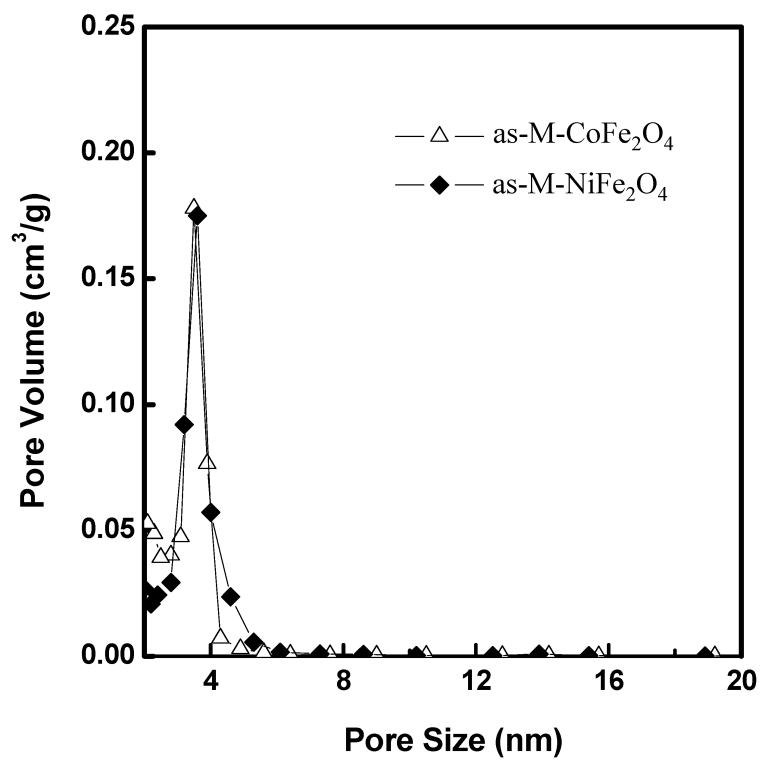


**Fig. S7** The pore size distribution of as-synthesized (a) M-CoFe<sub>2</sub>O<sub>4</sub> and (b) M-NiFe<sub>2</sub>O<sub>4</sub>.

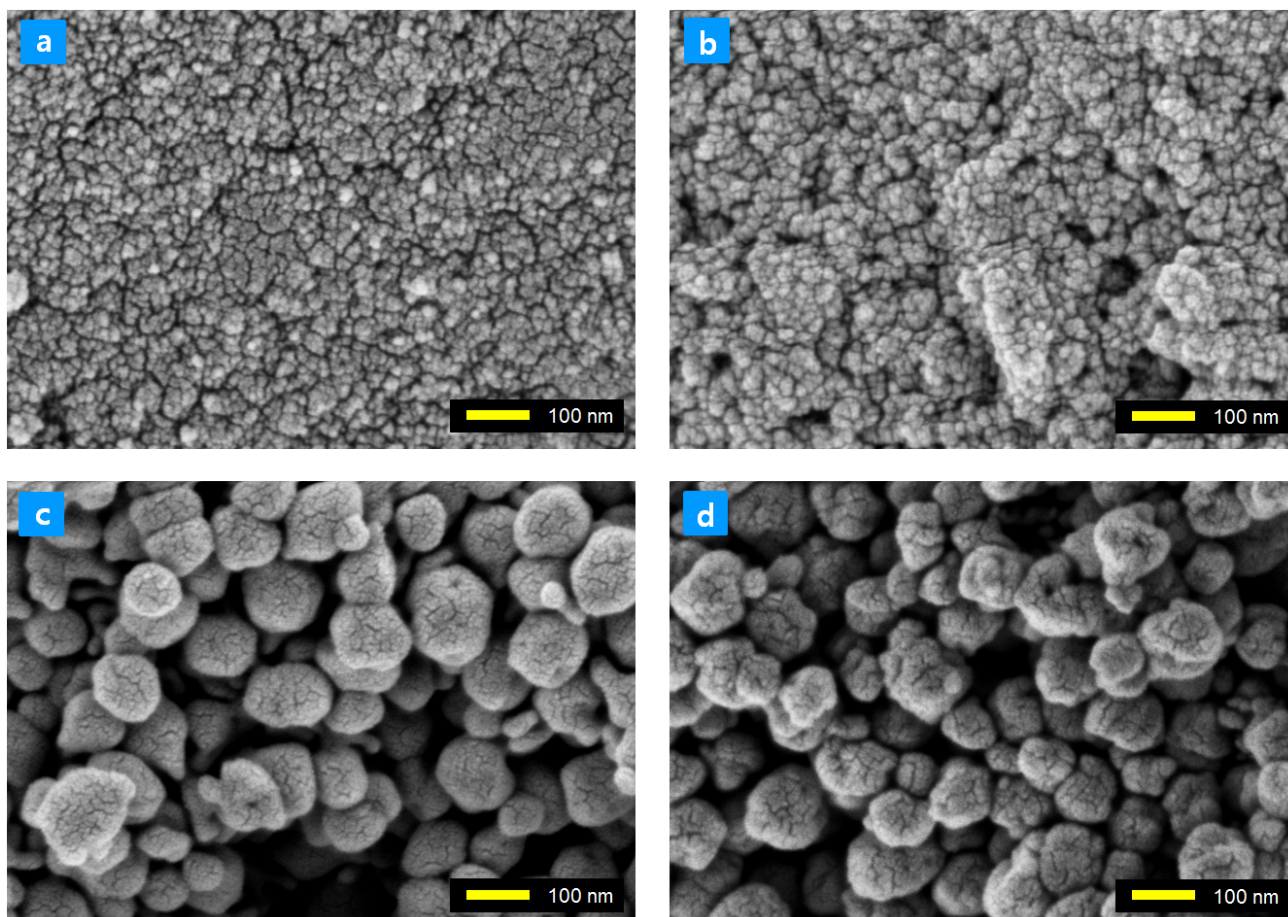


**Fig. S8** FE-SEM images of (a, c) CoFe<sub>2</sub>O<sub>4</sub> and (b, d) NiFe<sub>2</sub>O<sub>4</sub> at different sodium acetate concentrations; (a, b) high concentration and (c, d) low concentration.

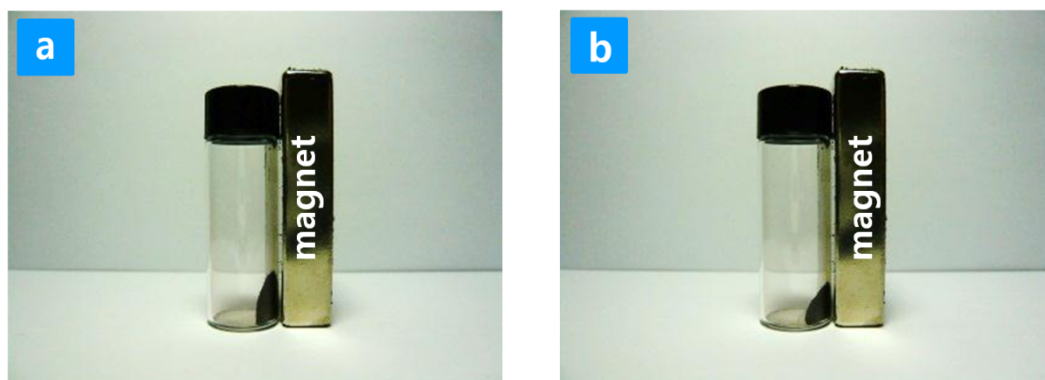


**Fig. S9** Photograph of (a) M-CoFe<sub>2</sub>O<sub>4</sub> and (b) M-NiFe<sub>2</sub>O<sub>4</sub> particles in the presence of a magnetic field.